ME4242 SOFT ROBOTICS
FINAL GROUP PROJECT REPORT

GROUP 1

CHEN XUN (A0237207J)

HANAA AMIRA SANTO (A0239117E)

HA ZHE LI (A0236541J)

TENG WEN SIAN ETHAN (A023338A)

WANG CHUN YI (A0239928L)

Contents

1. Introduction

1.1 Background on Hard Robotics and Soft Robotics

Traditional hard robots are characterized by their strict kinematic chain with rigid links and joints, commonly used in manufacturing. These hard robots are specifically designed for distinct, singular tasks and are usually not as versatile in other operations (Rus & Tolley, 2015). Hard robots are actuated repetitively and precisely, down to detailed specifications such as degrees of freedom.

In comparison to hard robots, soft robots are made of compliant materials allowing complex movements not attainable by traditional hard robots. Due to the lack of resistance to high forces of compression, soft robots have the flexibility to adapt its own shape to accommodate the obstacles in the robot’s path. This allows them to actuate without causing much damage to itself, as well as their surrounding area as it manoeuvres through obstacles. While hard robots typically dedicate one actuator per joint, soft robots consist of a fully integrated system, incorporating the actuators within the entire structure (Trivedi, et al., 2008).

In this final project, we were given the task of designing, building, and demonstrating an aquatic soft robot, which will be described in this report in more detail.

1.2 Design and Modelling of a Soft Robotic Fish Inspired by the Angler Fish

A particular area to be explored in soft robotics is the creation of aquatic soft robots, which has an abundance of advantages in ecological studies. Traditional methods of rotational propulsion mechanisms of large and rigid aquatic robots have proven to be of high disturbance to marine life, as it results in disturbances such as waves and vibrations within the water body. In the worst case, it may even pull in objects and wildlife into its propeller, entangling or endangering nearby marine species (Van Den Berg, Scharff, Rusak, & Wu, 2022).

In our aquatic soft robotics project, we are utilising oscillatory propulsions in our actuation, which eliminates all of the abovementioned issues of traditional rotational propulsion hard robots. With its soft actuation, it reduces the disturbances caused in the water and pushes water, objects, and marine life away from the robot, rather than pulling them in towards the robot. Its quieter movements and reduction in disturbances allows the robot to be useful in underwater exploration and observation of underwater marine life peacefully.

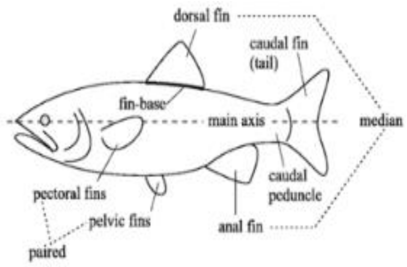

Figure 1: Diagram of a typical fish with labels (Lindsey, 1978)

Figure 1 presents a diagram of a typical fish body and a terminology of its associated parts. The swimming mechanism of fish in water involves the transfer of momentum from the fish body and the surrounding water. This paper will elaborate on the design of the caudal fin, swimming mode, and overall architecture of the soft robotic fish.

The key elements of soft robotics design and its applications to the specifications of the robot will be further explained in detail in the methodology section.

2. Methodology

2.1 Design and Fabrication

The overall design of the aquatic soft robot was inspired by a fish, with some physical characteristics of the fish adapted and used in the design. Some direct forms of biomimetics were utilised, such as the dangling lure of an angler fish, lunate caudal fin from tuna fish, and the thunniform mode of locomotion were incorporated.

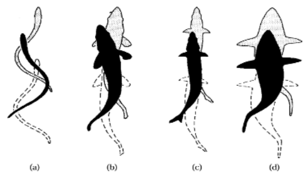

Figure 2: (d) Thunniform locomotion (Lindsey, 1978)

We have selected the thunniform mode of locomotion as it is the most efficient mode of locomotion (Sfakiotakis, Lane, & Davies, 1999). The aquatic soft robot features a larger fish body which was desirable as it could accommodate and enclose our electrical components. PLA, fabric thermoplastic polyurethane (TPU), and silicone of shore hardness 15 were used to fabricate our robot.

The following sections will outline the design considerations, fabrication methods used and the five key elements of soft robotics in actuation, modelling, control, sensing, and system integration.

2.1.1 Head

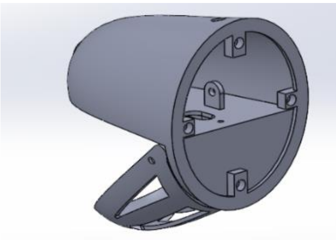

Figure 3: Head CAD model with 4 mounting holes for magnets

The head was designed in conjunction with the body, featuring a 3mm thick wall at 100% infill to reduce the permeability of water, and 3D-printed using PLA. While it was initially decided to use nuts and bolts to fasten the different sections (head, body, tail) together, there was difficulty in accessing the interior fastening points on the head. Hence, we modified the head-body connector to use magnets as a connector. Where the head meets the body, four 6mm deep holes were designed to house 8mm x 3mm neodymium magnets. The depths of the holes were dimensioned to accommodate the four magnets on the body, which slid into the holes in the head during magnetic assembly. Thereby, limiting movement via sliding and minimising shear force on the magnetic connection. This reduced the possibility of detachment, as the magnetic connections were significantly more resistant to tension than to shear forces. While the magnets themselves were insufficient to provide a waterproof seal even with an O-ring, it granted us easier access to the internal configuration during iteration and trials. In the final product, they hold the head in position while the waterproofing sealant cures.

Another feature is a 15 mm hole at the top of the head, designed to allow crucial electronics to be accessible after the joint has been sealed. These crucial electronics include the charging cable for the rechargeable battery, data cable for the Arduino, HC-06 Bluetooth module, and the LED light. This LED light is part of the robot fish's special feature and resembles that of an anglerfish's lure.

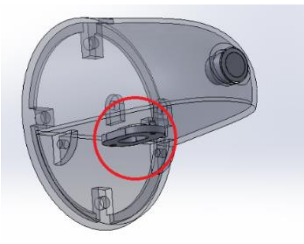

Figure 4: Flat piece for waterproof seal, location of eventual switch

We repurposed our unimplemented jaw opening and closing mechanism, which can be found in section 4.1. Its large head area was originally designed to house a solenoid that required significant space. Hence, the rounded cone design rather than a more traditional triangular one in popular images of fishes. This large space proved valuable for fitting the battery, various cables, and excess components. Thus, improving the balance and weight distribution of our robotic fish.

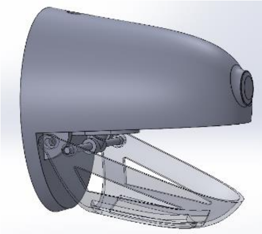

Figure 5: CAD Model of initial jaw mechanism

Another modification was to install a power switch within the waterproofed area for the original jaw actuation mechanism. It consisted of a rubber balloon wrapped around the flat piece shown in Figure 4, which was attached to the base of the head to create a waterproof seal that allows movement. This soft flexible area became the ideal location to install a rocker switch as it allows easy waterproof access, saving further design complications.

Finally, a 2mm thick PLA jaw was 3D printed via the modification of one half of the rounded cone shape of the head. It is attached via two pin joints at the sides of the head, with cutouts to reduce the weight of the jaw and overall robot as well as ease movement.

2.1.2 Body

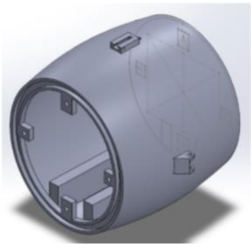

Figure 6: CAD Model of the fish body

Similarly, the body was 3D printed using PLA at an infill percentage of 60% and coated with a few layers of waterproof epoxy coating. To minimise weight and maximise the interior carrying capacity of the body, it featured a 3mm lofted surface with oval reference geometries. These reference geometries were made to accommodate a square interior measuring 80mm by 80mm, derived by measuring the total size of the internal components such as the fluidic control board, Arduino, pneumatic motor, etc.

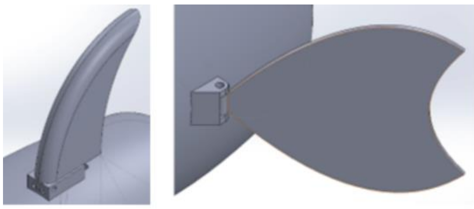

Figure 7: From left to right (a) Dorsal fin attached using dovetail joint, (b) Pectoral fin attached using pivot hinge

A set of pectoral, anal, and dorsal fins were attached to the body to aid in locomotion as well. The pectoral fins, actuated by balloons, provided propulsion for transient movements like turning, with actuation only necessary at specific moments (Vignesh, Asokan, & R, 2023). The anal and dorsal fins contributed to aquatic stability, by preventing the fish from rolling during locomotion.

To trial and test the effectiveness of different fin designs, the fin connectors were designed to be modular as seen from . The static anal and dorsal fins were attached using a dovetail joint and a 2mm securing pin, while the mobile pectoral fins were attached using a pivot hinge and an M3 plastic screw and nut set. An additional chamfer was also added to the hinge joint to reduce drag along the sides of the robotic fish.

Much like a high vacuum system, the joining mechanism between the body, head, and tail involved using a 130mm-5mm thick rubber O-ring, M3 screws, and nuts to secure the assembly. As seen in , there is a 4mm x 5.5mm (depth x width) groove extruded into the O-ring mount. This allows the O-ring to sit snugly and provide ample room for expansion during the securing process. Once the screws and nuts have been inserted into the assembly and tightened, the clamping force will cause the O-ring to deform and fill up the remaining gaps. After which, the exterior gap was waterproofed by applying 3 layers of waterproof epoxy spray and paste.

2.1.3 Tail

The tail was constructed using a combination of 3D printed PLA connectors at 60% infill density and a silicone mold. The PLA connector was precisely designed to fit the body, featuring 4 dowel holes that align with those on the body. Four 20mm long M3 screws were glued into place with threads facing the towards the body, so that they can be used to secure the tail to the body. According to our needs for a flexible silicone tail, silicone of shore hardness 15 was selected to balance flexibility and strength.

Figure 8: CAD model of the PLA connector (left), fully molded silicone tail (right)

However, since silicone does not bond well with PLA, we adapted a mechanical interlocking design in our tail connector as seen in Figure 8. The interlocking design, adapted from a University of Delft research paper (Rossing, Scharff, Chompff, Wang, & Doubrovski, 2019), features an extruded mesh of rectangles. These rectangles provided valleys for silicone to fill and cure, resulting in a strong mechanical attachment to the PLA connector. A 15mm by 30mm rectangular hole was also incorporated to fit a 90mm rectangular PLA insert, creating a cavity for the bending actuator.

Figure 9: Top view of the mold held down by F-clamps

To create the tail, we first designed an open PLA mold to house the PLA connector and silicone. The aft portion of the mold was intentionally smaller and thinner than the tail connector to reduce drag and resistance during underwater movement (Vignesh, Asokan, & R, 2023). Our fabrication process began by positioning the PLA connector with the rectangular PLA insert within the mold and sealing its extremities with tape. After which, four F-clamps – two laterally and two vertically – were used to secure the mold. The silicone was mixed at a ratio of 1ml activation agent to 100ml of silicone for 5 minutes and then poured into the mold. Once the silicone had filled the mold, the snap fit connector for the caudal fin was pushed into the silicone to complete the mold setup. After 24 hours, the mold was cured, and the tail was removed. Due to reasons listed in section 4.1, the silicone tail was then truncated to about 90mm by cutting off the excess silicone near the trailing end. Finally, two pneumatic tubes were routed out of the tail to connect directly to our bending actuator, and RTV was used to seal the gaps.

2.1.4 Caudal Fin

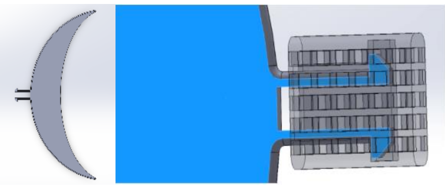

Figure 10: CAD Model of Caudal fin and snap fit connector

The thunniform mode of locomotion involves the transfer of momentum from its oscillating caudal fin to the surrounding water to drive the fish forward. As previously mentioned in the tail design segment, the aft tail portion was designed to reduce underwater drag. This in turn promotes flow to the caudal fin, greatly enhancing its thrust. To iterate and test different caudal fins, a snap fit connector was integrated for simple replacement of the caudal fin. To achieve a balance between thrust and efficiency, we chose to mimic the lunate design of a tuna's caudal fin (Vignesh, Asokan, & R, 2023). The lunate caudal fin has an aspect ratio of 5.7, a filleted leading edge for less drag, and was 2mm wide to retain flexibility in water.

2.1.5 Soft Fluidic Actuator

The first key element of soft robotics is the actuation mechanism, which provides the propulsive force for our soft-robotic fish.

Figure 11: Final bending actuator (left most), bending actuation as pouches are inflated (Following 3 images)

Our final actuator comprised of two pouches, made of TPU fabric measuring 5.5cm x 33cm, each arranged into two bellows. Their edges were sealed using fabric welding, a method of fabric adhesion achieved through heat treatment with a household iron. The actuation mechanism utilises positive pressure to inflate the expandable TPU pouches, which are taped to each side of a fixed uninflatable strip of TPU fabric. The two bellows were created using 3cm wide duct tape, such that the bellows closer to the body are smaller than that of the bellows nearer the caudal fin.

As seen in Figure 11 , upon inflation of the left pouch (comprising two parallel bellows), the actuator will bend to the right side. Conversely, inflating the right pouch causes the actuator to bend to the left. Once the caudal fin is attached, the generation of force transfers momentum to the surrounding water, resulting in the thunniform mode of locomotion for our robotic fish.

2.2 Simple Mathematical Model

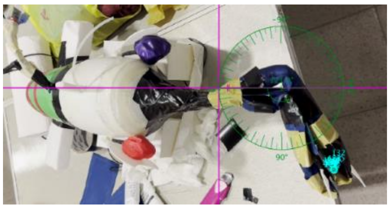

Figure 12: Tracking software measuring bending angle

The second key element of soft robotics is modelling, which is the understanding of the soft robotic mechanism. Our mathematical model will be mainly based on the bending angle model, as leaks and inconsistencies made it challenging to accurately measure force output. In mathematical model, we assumed that there were no leaks in the actuator and that the loss of energy through other means were negligible. Using a tracking software (Tracker) shown in Figure 12, the bending angle of the actuator was measured from a fixed pivot point. The software followed a point placed on the tail using an auto tracker, measuring the bending angle of the tail over a few oscillations. We then developed a model, illustrated in , that could predict the bending angle of the tail under varying pneumatic pressure inputs.

2.2.1 Pressure-Bending Angle Model

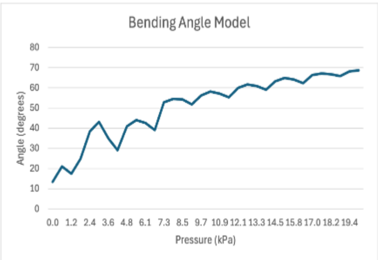

Figure 13: Pressure-Bending Angle Model

As our fish was propelled by its tail, we wanted to ensure that the angle of the tail was sufficient to push against the water to propel itself forward. Since the optimal angle of oscillation is 35 º (Vignesh, Asokan, & R, 2023), we wanted to identify the necessary pressure range and inflation duration needed to achieve such actuation. Thus, we modelled the bending angle against pressure to identify the optimal parameters.

$$\boldsymbol{P} = \frac{2kl^2\theta_1}{\pi w(r^2 - L^2 - r^2{\theta_1}^2 - 2rL\theta_1)}$$

Total bending angle = 2(n-1)θ_1

Figure 14: Formula of relationship between Pressure and Bending Angle

As seen in , pressure input is proportional to bending angle; The greater the pressure, the greater the bending angle. However, at higher pressures, our TPU fabric actuator was prone to bursting, leading to leakages. Thus, we were only able to model the bending angle of the tail below the maximum pressure input of 20kPa. At this maximum pressure, it could bend to a maximum angle of around 70º. As we expected, as we approach the maximum pressure, the rate of change of bending angle decreases, ultimately reaching its maximum bending angle.

Next, we utilised other elements of the bending angle model to allow actuation to closely mimic that of a fish. As we are using bellow-based actuators for our tail, we will be estimating the total bending angle using the following equation in .

$$\theta = tan^{-1}(\frac{y_{max}}{0.5b})$$

$$\theta_{total} = 2(n-1)\theta$$, *where n = number of bellows*

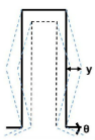

Figure 15: Bellow based equations

Our initial iterations of the bending actuator included three bellows with two inter-bellow tapes, but the bending angle of the actuation was greater than those of a common thunniform locomotion. At a fixed length of 20cm and with more than 2 bellows, the height b would be smaller. Assuming the Ymax expansion, shown in , is the same at a fixed pressure, the bending angle will increase, increasing the overall bending angle as well, due to a larger n value. This resulted in the pivoting of the robotic fish instead of moving forwards. Hence, we reduced the number of bellows to two, which was sufficient to achieve the desired bending angle.

2.2.2 Pressure-Force Model

Estimating Force from Pressure

$$F_{max} = \frac{P \times ab \times y_{mean}}{L \times tan^{-1}(\frac{y_{max}}{0.5b})}$$

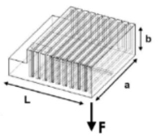

Figure 16: Equations for estimating force from pressure

Lastly, we also utilised the force-torque model where we experimented with the variables in to adjust the force exerted by the actuator. This was to ensure there is sufficient force to push against the water pressure to move forward.

We experimented on increasing the width of our actuator (variable *a* in), which was initially between a 3cm - 5cm diameter, to increase the force output (ab increases, F max increases). While decreasing the length of the actuator would help in increasing the force output (L decreases, Fmax increases), it was not possible to shorten the actuator further. A shorter length would result in kinks in the TPU fabric forming a curved bellow, restricting the airflow within the actuator and preventing it from bending.

To achieve the best bending actuation, we have used our mathematical model to trial and test various positions where the inter-bellow tape should be placed. After experimentation, we have found that the best setup was to create a smaller bellow nearer to the body of the fish, and a larger bellow closer to the end of the tail. This allows the actuator to flick into the optimal position with sufficient force, allowing our actuator to push the water away and propel the fish forward.

2.3 Control

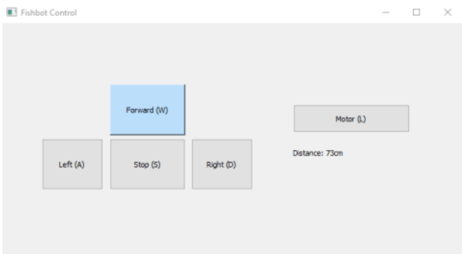

Figure 18: PyQt5 Graphical User Interface

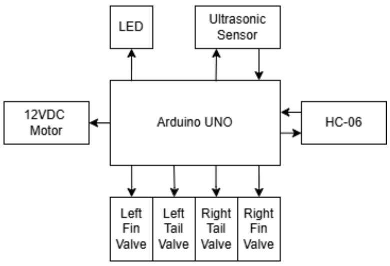

Figure 18: Block diagram of electrical

The third key element of soft robotics is control. To achieve movement and obstacle detection, we used an Arduino UNO microcontroller to control several components shown in Figure 18. To allow for wireless communication, we added a HC-06 Bluetooth Module and wrote a Python script to send and receive messages from the Bluetooth serial. The robot movements are then controlled using a laptop keyboard input along with a PyQt5 Graphical User Interface (GUI) to display the current motion. For codes used in this project, please click here to view the Github repository.

All the components were powered with a rechargeable 12V Lithium-ion battery. With some simple power calculation in a worst-case scenario (all components are always on), we expect our hourly current draw to be roughly 1530mA. A 1800mAh battery was hence chosen to ensure sufficient operation time yet minimising weight for buoyancy.

2.3.1 Movement

We have designed our robot to be able to achieve four types of motion – forward, left, right, and stop. This was done by controlling the air supplied to each actuator using pneumatic valves. Actuation was achieved using four L-port 3-way valves. A 12VDC pneumatic pump was used to supply air to the actuators. Due to difficulties in making the actuators perfectly leak proof, we chose to keep the fluidic circuit open, drawing air from the external environment to inflate our actuators. To dispel air from the pectoral fin actuators, we made use of the intrinsic elasticity of the balloons to push the air out when inactive. As for the fabric tail, the actuation of either side was mutually exclusive, meaning that when one side of the tail is actuated with positive pressure, the other side will not be supplied with any air. This allowed the air from the non-actuating side to be pushed out by the force generated by the actuating side.

Forward motion was achieved using the TPU tail. As described in Section 2.1.5, the robot can be propelled forward by alternating the inflation of the left and right pouches in the tail at equal intervals. Turning was achieved using both the tail and the pectoral fins. To turn left, we supply air to the balloon on the left fin to open the fin outwards and create more drag on the left side, causing our robot to pivot. At the same time, we supply air to the right pouch on the tail to bend the tail leftwards, pushing the fish to the left. To return the tail to its centre position, the left pouch is inflated for a much shorter duration. To turn right, the same sequence is done on the inverted side. To stop the robot, we open both pectoral fins to create as much resistance against forward motion as possible and turn off the pump after the two balloons are fully inflated.

To avoid instability caused by dropped packages during Bluetooth communication, we split the motion loops between the Arduino code and the python script. Instead of turning each valve on and off from a Bluetooth serial instruction, the required sequence of motion for one loop is written in the Arduino code. This sequence will run every time its corresponding command is sent from the Python script, reducing the communication overhead and avoiding dropped packages due to an overloaded Bluetooth serial. Moreover, due to the handmade nature of our fluidic actuator, the two sides may not always produce the same amount of bending even when supplied with the same amount of air. Hence, we adjusted the inflation time accordingly. We also made use of Pulse Width Modulation (PWM) to control the output from our pump, preventing leaking or bursting caused by excessively high pressures.

2.3.2 Ultrasound Obstacle Detection

The fourth key element of soft robotics is sensing, which was how our robot interacts with the given environment. This sensing mechanism was adopted for our soft robot’s special ability.

For this purpose, a sonar detection method was utilised in the ultrasonic transducer for obstacle detection. It sent a square wave signal and detected any return signals due to reflection from obstacles from the pulse. The time taken for the return pulse would allow for calculation of distance from the sensor to the obstacle. It has a range of 25 to 450cm and an effective angle of 50°. Threading was implemented in our Python script to display the output of this sensor in the GUI without the window freezing up.

The LED light on our robotic fish had been set to light up when an obstacle is within 60cm. A 62ohm resistor was added to prevent excessive current draw from the LED as that could lead to other components malfunctioning due to insufficient power.

2.4 Experimental Protocol

The last key element of soft robotics is our system integration. Through experimentation and iterating, we rectified issues and optimized the performance of our robotic fish.

Figure 19: Electronics fitted into body

The head, body, and tail segments were seamlessly joined to enclose our electronics within a waterproof shell. O-rings were first positioned within the grooves on the body, followed by the attachment of the tail using four sets of M3 screws and nuts. The gap between the tail and body was further waterproofed by three layers of silicone and epoxy waterproofing spray. Tubes were extended out of the tail and body for attachment to respective actuators in later assembly, the gaps were also sealed using epoxy.

We soldered most of the wires to our PCBs and secured the rest of the pins using hot glue. Tubing assemblies were reinforced with electrical tape and secured with heat shrink to reduce the possibility of leakages. We layered our electronics within the body of the actuator, using soft vacuum bags and cardboard placed within empty gaps to ensure that all electronics were sat in place with little movements. The heavier items such as the pneumatic motor and valves were placed at the bottom to lower the centre of mass, followed by the Arduino connected to the fluidic control board, and finally the ultrasound board at the top. The HC-06 Bluetooth module, LED light, Arduino cable, and battery charging cable were routed out through the head for the ease of accessibility.

Figure 20: Final Fish Robot

Once the placement of the wires and cables were complete, our system was tested once more to check its functionality. After which, the head was joined to the body using neodymium magnets and similarly sealed with layers of silicone and epoxy waterproofing spray. As an additional failsafe, flex tape was applied on the head-body and body-tail joints, creating an extra layer of waterproofing. Upon completion, the robotic fish was waterproof except the portion of the head with a hole for our cables.

The robotic fish was placed in the water first to check buoyancy and rolling, with different sizes of anal fins attached. After which, we began testing and optimising the control of the robotic fish in the water. This was accomplished by testing different iterations of the bending actuators by varying bellow lengths, fin sizes, as well as PWM and inflation durations to the various actuators.

3. Results and Discussion

Overall, our robotic fish demonstrated its ability to float, move forwards, turn left, turn right (with some difficulty) as well as to sense obstacles within a 60cm radius. The methods for waterproofing, securing electrical, and pneumatic connections proved highly effective, as there were no functional issues with the robotic fish after it was sealed. illustrates the results. Figure 21 illustrates the results.

Our bending actuator, although imbalanced, was able to provide the necessary propulsion force for our aquatic motions. The imbalance was due to wear and tear, as there were more holes in the left pouch (from the rear view) than in the right pouch, causing it to inflate less for a given duty cycle.

Figure 21: From left to right, robotic fish swimming forwards, turning left, turning right, LED lighting up near obstacles

As seen from Figure 21, where the red arrows indicate direction of motion, we were able to achieve forward motion consistently by inflating the left pouch slightly longer than the right pouch. As mentioned in 2.3.1, this balanced the oscillation and consequently the forward propulsion of the robotic fish.

On the one hand, since the right pouch was stronger than the left, turning left was easily achieved as the tail would naturally bend left. The left turning action by the left fin and leftward motion of the tail is indicated by the orange line and curve on the second image from the left in Figure 21.

On the other hand, turning right was much more difficult as we needed a longer inflation time for the left pouch to push the tail in the other direction. This issue was exacerbated by the lack of vacuum in our system, which meant that the already inflated right pouch provided resistance to the inflation of the left pouch. Thus, our motor would often stall or failed to inflate the left pouch enough to generate enough bending motion, leading us to reset the tail's position in the water.

Otherwise, the special ability of our robotic fish to light up an LED upon detecting obstacles functioned flawlessly. This feature was strongly visible at night and provided immediate visual feedback of the fish's surroundings.

Regardless of the size of the anal fin, it could not stop the round and regular fish body from rolling. Thus, a Styrofoam stabiliser was added in the jaw to prevent rolling. The routing of the Arduino cable, charging cable, and HC-06 Bluetooth module out of the head also provided us easy access to modifying our code to improve and optimise control of the robotic fish.

4. Limitations and Improvements

4.1 Limitations

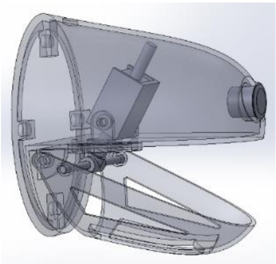

Figure 22: Initial jaw mechanism CAD model

While our robotic fish could float without the help of external attachments, weight was one of the limiting factors that we had to deal with. The initial design included a jaw opening and closing mechanism, mainly driven by a solenoid or some sort of cable actuators, as seen in . This mechanism would react to the presence of a nearby object and clamp down on it to imitate hunting and biting. However, considering the heavy PLA head due to a 100% infill density and the additional weight that would be added to the robot, it would inevitably cause a larger portion of the fish to submerge. Hence, posing an issue for our control and waterproofing. Additionally, the presence of linkages and moving parts made of hard materials dictated the need for a flexible waterproof material to allow ease of movement, while covering the entire mechanism to ensure there are no gaps during actuation for water to seep in. Such a design is space intensive and cumbersome in implementation.

Another issue was the balance between modularity and waterproofing of the robot. As the robot should ideally be mostly submerged underwater for effective locomotion, it necessitates good waterproofing to prevent water from damaging the internal circuitry. This meant using waterproof sealants like RTV which not only have a long curing time of 24 hours, but also were troublesome to remove when iterating on our design. This created a time constraint which greatly reduced our time to iterate and test different configurations.

Moreover, many iterations of the actuator had led up to the final model. Our initial design included a silicone tail to house the bending actuator to avoid this issue. However, after testing, the silicone tail was too stiff to be actuated by the low force pneumatic bending actuator. As a result, we had to shorten the tail and use the bending actuator directly in the water. We had also previously tried different types of household poly vinyl chloride (PVC) sheets sealed with either soft plastic glue, super glue, hard plastic, soldered edges, flex tape, or duct tape to no avail. The bonding strength of the adhesives or seals were insufficient to withstand the pressure from our pneumatic motor. These actuators failed tests of retaining 22 Pa of pressure in the bio-robotics lab. Additionally, chlorine is a strong oxidiser, which further breaks down adhesives and reduces the strength of the seal. Ultimately, we have found out that actuators fabricated using adhesives should not be exposed to chlorine water.

The robotic fish also displayed a slow speed of motion in water. Firstly, as our robotic fish was half submerged, only about half of the fins were submerged in the water. This led to a reduced transfer of momentum to the surrounding water and a lack of propulsive force from its tail. To improve the force output of the bending actuator in the water, some plastic sheets were added to the tail. Hence, allowing the robotic fish to transfer more momentum to its surrounding water and move slightly faster. Secondly, the limited expansion of the pectoral fin balloons also hampered our movement speed, as they were only pushing small volumes of water to assist in turning or coming to a stop. Finally, incorporating the Styrofoam stabiliser in the jaw prevented rolling of our body, but introduced greater aquatic drag. Consequently, it required more power from the already weak bending actuator to propel the robotic fish forwards, which accelerated its degradation. Ultimately, the bending actuator was inoperable on the day of the showcase.

4.2 Future Works

For a partially submerged robotic fish, the weight issue can be circumvented by adjusting and finding the optimal settings for creating waterproof 3D prints, which include infill density, layer heights, wall thickness, and filament types. As proven by our project, it is possible to achieve a waterproofed PLA body with an infill density of 60% by layering the exterior with waterproof epoxy. Thus, creating a lighter and larger body whilst retaining the needed strength for greater underwater efficiency. This will enable more features, such as the actuating jaw or a larger battery, to be incorporated into the final robotic fish.

To address the difficulty of waterproofing linkages and moving parts, from our experiences, one of the improvements could be to use a soft actuation method such a pouch motor for bending. It will be more efficient for our use case of low-pressure underwater actuation, as the only additional point of sealing would be between the inlet fluidic tube and the body rather than a whole mechanism.

After our lack of success in fabricating a durable bending actuator using household plastics, the actuator could be 3D printed with TPU or fabricated using mold casted silicone. The slight flexibility of these materials would allow some room for expansion during inflation, improving its resistance to pressure and solving our leakage problems. Furthermore, a 3D printed, or a silicone mold casted actuator would be more durable and would have fewer mechanically weak points due to the lack of seams or adhesive seals. This bending actuator can then be housed in a thinner skin like layer of silicone, which will protect it from the environment and prolong its lifespan.

Our robotic fish has potential for a fully submerged model. This can be accomplished by fabricating a reliable bending actuator, waterproofing enhancements for a charging point and connection point to the internal circuitry, an air bladder integration for buoyancy control, and pectoral fin adjustments to account for underwater lift and work in conjunction with the actuating tail. These improvements will enhance the overall manoeuvrability and efficiency of the robotic fish, allowing it to delve deeper into marine ecosystems and explore marine life.

5. Conclusion

In summary, our group has successfully constructed an enclosed, untethered, waterproof soft robotic fish capable of moving forwards, turning left and right, as well as detecting obstacles using an ultrasound sensor in its head. While we faced challenges in fabricating a durable bending actuator, balancing waterproofing and modularity, and achieving fast swimming speeds, we have proposed several improvements. These include adjusting printing density and settings, 3D printing a bending actuator using TPU, and exploring further advancements to enhance the overall performance and efficiency of the robotic fish. With these advancements, we aim to enable the robotic fish to explore marine ecosystems more effectively.

6. Bibliography

Lindsey, C. C. (1978). Form, function and locomotory habits in fish. In W. S. Hoar, & D. .. Randall, *Fish Physiology Vol. VII Locomotion* (pp. 1-100). New York: Academic.

Rossing, L., Scharff, R. B., Chompff, B., Wang, C. C., & Doubrovski, E. L. (2019). Bonding between silicones and thermoplastics using 3D printed mechanical interlocking. *Materials and Design*.

Rus, D., & Tolley, M. T. (2015). Design, fabrication and control of soft robots. Retrieved from http://dx.doi.org/10.1038/nature14543

Sfakiotakis, M., Lane, D. M., & Davies, J. B. (1999, April). Review of Fish Swimming Modes for Aquatic Locomotion. *IEEE JOURNAL OF OCEANIC ENGINEERING, 24*(2).

Trivedi, Deepak, Rahn, Chris, Kier, William, & Walker, I. (2008). Soft Robotics: Biological Inspiration, State of the Art, and Future Research. *Applied Bionics and Biomechanics*, 99-117. doi:10.1080/11762320802557865

Van Den Berg, S. C., Scharff, R. B., Rusak, Z., & Wu, J. (2022). OpenFish: Biomimetic design of a soft robotic fish for high-speed locomotion. *HardwareX*.

Vignesh, D., Asokan, T., & R, V. (2023). Performance analysis of a caudal fin in open water and its coupled interaction with a biomimetic AUV. *Ocean Engineering*.

7. Appendices

7.1 Individual Contributions

Group Member	Contributions
CHEN XUN (A0237207J)	2.1.1 Head 4. Limitations and Improvements
HANAA AMIRA SANTO (A0239117E)	2.1.5 Soft Fluidic Actuator 2.2 Simple Mathematical Model
HA ZHE LI (A0236541J)	2.3 Control 7. Appendices
TENG WEN SIAN ETHAN (A023338A)	All sections
WANG CHUN YI (A0239928L)	1. Introduction 2.1.5 Soft Fluidic Actuator 2.2 Simple Mathematical Model 7. Appendices

7.2 Bill of Materials (BOM)

Item	**Quantity**
3D-Printed Components	
Body and head	1
Variety of fins	5
Actuator Soft Materials	
Balloons	2
TPU fabric fluidic actuated tail	1
Electronics	
Arduino UNO	1
Fluidic Control Board V5.0	1
D2028B 12V Airpo vacuum pump	1
12V 1800mAh rechargeable battery	1
Mini 3-way pneumatic valves	4
HC-06 Bluetooth module	1
JSN-SR04T waterproof ultrasonic sensor	1
Standard 5mm yellow LED	1
Solder breadboard	2
1k ohm resistor	3
62-ohm resistor	1
On-off rocker switch	1
Waterproofing and Adhesive	
Silicone sealant (200ml)	1
Waterproof spray (450 ml)	1
Plastic Adhesive (50ml)	1
Super glue (20ml)	1
Miscellaneous Off-the-shelf Parts	
130mm-5mm O-ring	2
M3 nut and bolt	4
M3 plastic nut and bolt	2
5-way push-in tubing connector	2
8mm x 3mm neodymium magnets	8
Pneumatic tubing 6 mm by 5 mm (2m)	1

7.3 Bending Actuator Iterations

Figure 23: First iteration of 3cm diameter bending actuator with PVC plastic and soft plastic glue.

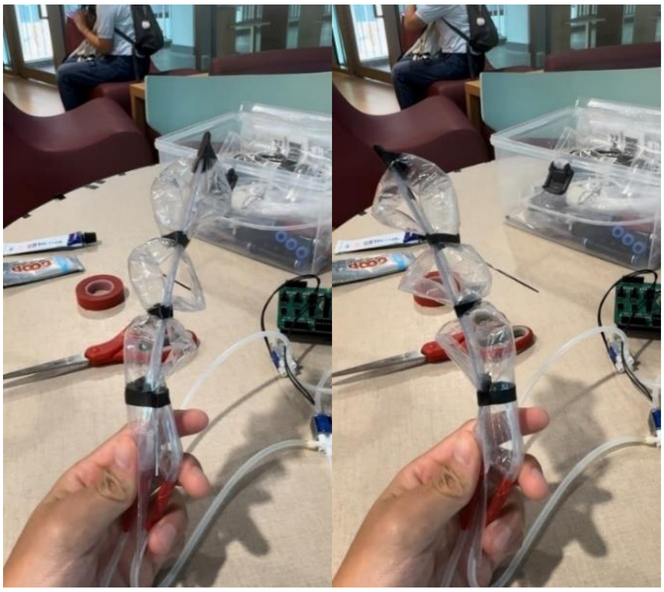

Figure 24: Iteration of 3cm diameter bending actuator with PVC plastic and adhesive silicone.

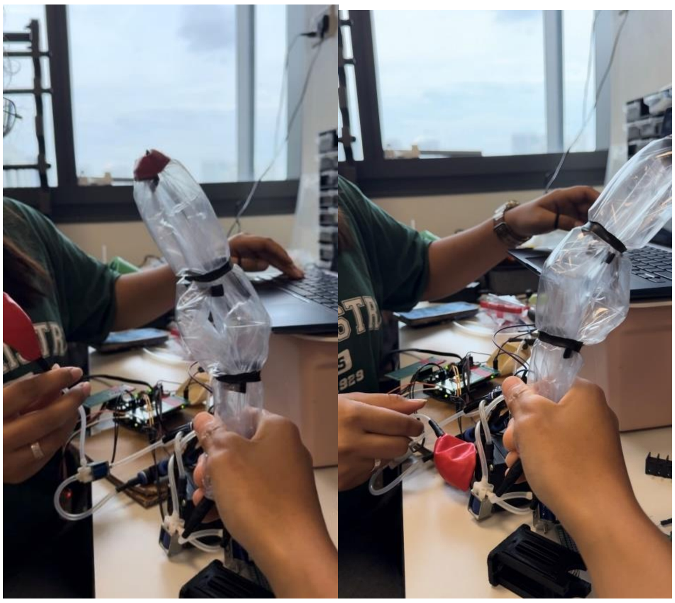

Figure 25: Iteration of 5cm diameter bending actuator with PVC plastic and plastic glue.

Figure 26: Iteration of bending actuators with PVC plastic sealed using a soldering iron (left), iteration of bending actuator with TPU fabric sealed with a regular household iron.